

Marquette University

e-Publications@Marquette

---

Biological Sciences Faculty Research and  
Publications

Biological Sciences, Department of

---

9-1999

## Segmental Distribution of Common Synaptic Inputs to Spinal Motoneurons During Fictive Swimming in the Lamprey

James T. Buchanan

*Marquette University*, james.buchanan@marquette.edu

Stefan Kasicki

*Marquette University*

Follow this and additional works at: [https://epublications.marquette.edu/bio\\_fac](https://epublications.marquette.edu/bio_fac)



Part of the [Biology Commons](#)

---

### Recommended Citation

Buchanan, James T. and Kasicki, Stefan, "Segmental Distribution of Common Synaptic Inputs to Spinal Motoneurons During Fictive Swimming in the Lamprey" (1999). *Biological Sciences Faculty Research and Publications*. 162.

[https://epublications.marquette.edu/bio\\_fac/162](https://epublications.marquette.edu/bio_fac/162)

Marquette University

**e-Publications@Marquette**

***Biological Sciences Faculty Research and Publications/College of Arts and Sciences***

***This paper is NOT THE PUBLISHED VERSION; but the author's final, peer-reviewed manuscript.*** The published version may be accessed by following the link in the citation below.

*Journal of Neurophysiology*, Vol. 82, No. 3 (September 1999): 1156-1163. [DOI](#). This article is © American Physiological Society and permission has been granted for this version to appear in [e-Publications@Marquette](#). American Physiological Society does not grant permission for this article to be further copied/distributed or hosted elsewhere without the express permission from American Physiological Society.

# Segmental Distribution of Common Synaptic Inputs to Spinal Motoneurons During Fictive Swimming in the Lamprey

James T. Buchanan

Department of Biology, Marquette University, Milwaukee, Wisconsin

Stefan Kasicki

Department of Biology, Marquette University, Milwaukee, Wisconsin

## Abstract

These experiments were designed to measure the degree of shared synaptic inputs coming to pairs of myotomal motoneurons during swimming activity in the isolated spinal cord of the lamprey. In addition, the experiments measured the decrease in the degree of shared synaptic inputs with the distance between the motoneurons to assess the segmental distribution of these shared inputs. Intracellular microelectrode recordings of membrane potential were made simultaneously on pairs of myotomal motoneurons during swimming activity induced with an excitatory amino acid. The swim cycle oscillations of motoneuron membrane potentials were removed with a

digital notch filter, thus leaving the fast synaptic activities that underlie these slower oscillations. Cross-correlations of the fast synaptic activities in two simultaneously recorded motoneurons were made to measure the degree of shared inputs. The cross-correlation was done on time windows restricted to one swim cycle or to part of a swim cycle, and 50 consecutive swim cycle cross-correlograms then were averaged. The peak coefficients of the cross-correlations exhibited a wide range, even for pairs of motoneurons located near one another (range = 0.06–0.74, for pairs located within 2 segments). This observation suggests that there may be different functional classes of myotomal motoneurons with inputs originating from different sets of premotor interneurons. In spite of this variability, the mean peak correlation coefficients of motoneuron pairs clearly decreased with the distance between them. With separations of more than five segments, there was little or no clear correlation between the motoneurons (range = 0.04–0.10). These results suggest that common synaptic inputs to motoneurons during fictive swimming originate from local premotor interneurons and that beyond five spinal segments, common premotor inputs are rare or weak to motoneurons. Thus the premotor signals originating from the locomotor network have relatively short distribution lengths, on the order of 5 segments of 120 total spinal segments.

## INTRODUCTION

The lamprey, a primitive vertebrate fish, swims forward with lateral body waves that propagate from head to tail. The spinal cord contains the central pattern generator (CPG) for swimming as shown by exposure of the isolated spinal cord to an excitatory amino acid such as glutamate. Under these conditions, the spinal cord exhibits rhythmic alternating ventral root bursting (i.e., fictive swimming) similar to the pattern of electromyographic activity observed during intact swimming (Cohen and Wallén 1980; Wallén and Williams 1984). As few as two to three spinal segments isolated from any rostrocaudal level of the spinal cord can generate rhythmic bursting, so the CPG for swimming is proposed to be a continuous network of rhythm generators that can be reduced to a minimum unit oscillator of two to three segments. In this model, each unit oscillator generates the basic alternating pattern of activity between motoneurons on opposite sides of the spinal cord, and coupling among the unit oscillators by interneurons produces the head-to-tail propagation of the rhythmic activity characteristic of forward swimming (Cohen et al. 1992; Grillner et al. 1991, 1995). The present study addresses the segmental distribution lengths of synaptic outputs from the locomotor network to motoneurons.

On the basis of intracellular recordings from pairs of spinal neurons (Buchanan 1982, 1986; Buchanan et al. 1989), a network for the unit oscillator in the lamprey has been proposed (Buchanan 1986; Buchanan and Grillner 1987). Modeling studies have demonstrated that the proposed network can generate rhythmic activity with the appropriate phase relationships among motoneurons and interneurons (Buchanan 1992; Grillner et al. 1988; Wallén et al. 1992). The three types of interneurons of the network are known to have multisegmental axonal projections (Buchanan 1982; Buchanan et al. 1989; Rovainen 1974), and two of these, the CC interneurons and the excitatory interneurons, have direct outputs to motoneurons. Therefore these interneurons have been proposed to be responsible not only for rhythm-generation activity but also for interoscillator coupling and for premotor inputs to motoneurons. Modeling studies have demonstrated the feasibility of this proposal (Buchanan 1992; Williams 1992). In these models, the interoscillator coupling consists of spread of the same synaptic connectivities found within the unit oscillator to neighboring oscillators. The synaptic strengths of these connections are modeled to be greatest within the oscillator of origin and then to decline with distance from that origin (Williams 1992). This is supported by split-bath experiments in which measurements were made of the amplitudes of the summed excitatory and inhibitory synaptic inputs to motoneurons projecting from a fictively swimming half of spinal cord into a passive half. These experiments demonstrated a decline in synaptic amplitude with the distance from the active half up to eight segments from the diffusion barrier (Dale 1986).

The length of the interoscillator coupling signals in the lamprey is not known with certainty. A theoretical analysis of coupled oscillators, which has been applied to the lamprey locomotor system, has assumed that the interoscillator coupling signals are weak and occur only between nearest-neighbor oscillators (Williams et al. 1990). However, correlational analysis of ventral root discharges during fictive swimming has suggested that long-range coupling also may be present in the lamprey spinal cord (Mellen et al. 1995). In addition, experiments in which activity in intervening middle segments of spinal cord were blocked with low calcium or with inhibitory transmitters have demonstrated that detectable coupling can be achieved between fictively swimming regions separated by  $\leq 20$  segments (Miller and Sigvardt 1996; Rovainen 1985).

One approach to determining the functional lengths of the intersegmental coupling signals would be to compare the degree of similarity in synaptic inputs during fictive swimming to neurons separated by various distances. Rhythmically active neurons located in the same segment are presumably controlled mainly by the unit oscillator of that same segment but also may be influenced by the spread of synaptic connections from unit oscillators located in other segments. Thus two related neurons separated by several segments should have a subset of common synaptic inputs originating from the same unit oscillator, even though the two neurons each receive their strongest inputs from different unit oscillators. The distribution lengths of these common inputs should be measurable by making cross-correlations of the synaptic activities in neurons during fictive swimming. The present study takes this approach, focusing on the correlation of synaptic inputs to pairs of motoneurons. Although the motoneurons have not been considered to be a part of the rhythm-generating network (Wallén and Lansner 1984; but see Perrins and Roberts 1995), they do receive excitatory and inhibitory inputs from the network and therefore may reflect the distribution lengths of synaptic output from the network. It is possible, though, that the segmental distribution lengths of outputs from the locomotor network may be different for rhythm-generating interneurons compared with motoneurons. As a first step, the present study sought to measure the segmental distribution of common synaptic inputs to motoneurons occurring during fictive swimming by using intracellular recordings of membrane potential from pairs of motoneurons separated by various distances. The results indicate that the spread of signals from the unit oscillators to motoneurons occurs over relatively short distances, about five segments.

## METHODS

### Preparation and dissection

The experiments were done on seven adult silver lampreys (*Ichthyomyzon unicuspis*), 18–30 cm in length. The animals were anesthetized by immersion in a 0.01% solution of tricaine (3-aminobenzoic acid ethyl ester) (Sigma) until reflexes were lost. The animals then were decapitated, the brain destroyed mechanically, and a spinal cord/notochord preparation dissected in cooled Ringer solution as previously described (Rovainen 1974). The lengths of the preparations ranged from 15 to 56 spinal segments. Four of the preparations were between 46 and 56 segments in length, extending from midgill to the beginning of the fin; one preparation was 35 segments in length, and three were 15 segments in length. The four shorter preparations were taken from the midbody region between the last gill opening and the beginning of the fin. Each preparation was pinned to the silicone elastomer (Sylgard)-lined bottom of an experimental chamber which was perfused with cooled Ringer solution (8–9°C) at a rate of 2–4 ml/min. The Ringer solution consisted of the following (in mM): 91 NaCl, 2.1 KCl, 2.6 CaCl<sub>2</sub>, 1.8 MgCl<sub>2</sub>, 4 glucose, and 20 NaHCO<sub>3</sub>. The solution was continuously bubbled with 98% O<sub>2</sub>-2% CO<sub>2</sub> (pH 7.4).

### Recording techniques

Fictive swimming was induced in the spinal cord/notochord preparation by bath perfusion with *N*-methyl-d,l-aspartate (NMA) (0.2–0.3 mM) or with d-glutamate (0.5–0.7 mM). Swim activity was monitored with extracellular ventral root recordings made by placing the tip of a suction electrode onto a ventral root at its exit

point from the spinal cord. The membrane potentials of motoneurons were recorded with intracellular microelectrodes consisting of micropipettes filled with 4 M potassium acetate. The motoneurons ( $n = 78$ ) had action potentials of  $\geq 80$  mV in amplitude and were identified by the presence of one-for-one spikes in the nearby ventral root while eliciting intracellular action potentials with current injection. A total of 62 ipsilateral pairs of motoneurons were recorded (Fig.1A). In most experiments, an intracellular recording was maintained in one motoneuron while the second intracellular electrode was used to impale several other motoneurons. In two experiments, a single motoneuron was impaled simultaneously with two microelectrodes (Fig. 3A). These dual impalements were accomplished under visual control by virtue of the visibility of the cell bodies in the lamprey spinal cord using a stereomicroscope. All intracellular recordings of motoneurons were done within the midbody region to ensure that the cells were myotomal motoneurons and not fin motoneurons. Recordings were done in current-clamp bridge mode using an Axoclamp-2A amplifier (Axon Instruments). The bath fluid level was kept as low as possible over the spinal cord to minimize electrode capacitance, and a grounded aluminum foil shield was placed between the two intracellular electrodes to minimize interelectrode coupling.

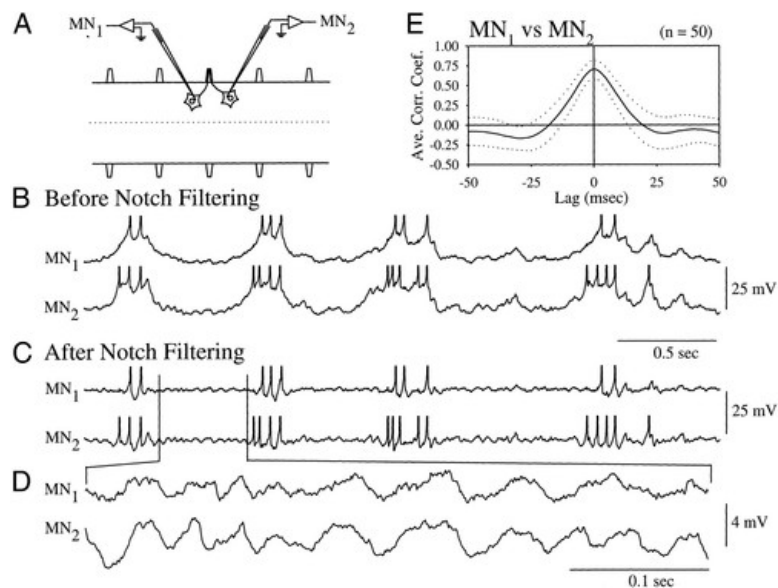


**Fig. 1.** Method for measuring cross-correlation of fast synaptic activity between pairs of motoneurons during fictive swimming. *A*: in this example, the membrane potentials of a pair of myotomal motoneurons ( $MN_1$  and  $MN_2$ ) projecting their axons out the same ventral root and separated by 0.5 segments were recorded simultaneously in a spinal cord/notochord preparation using intracellular microelectrodes.  $\cdots$ , midline of the spinal cord. *B*: during fictive swimming, the membrane potentials of the 2 motoneurons exhibited slow oscillations occurring at the swim cycle period that are the result of alternating phases of excitatory and inhibitory synaptic inputs. Action potentials occurring at the peaks of the slow depolarizations are truncated. *C*: using a digital notch filter, the slow membrane potential oscillations of fictive swimming were removed. Cross-correlograms then were calculated between the 2 filtered membrane potential records using windows of either single swim-cycles or, if spikes were present, of regions between spikes (e.g., the region between  $\parallel \parallel$ ). *D*: a higher gain display of the indicated region of *C* to show the synaptic activity in the 2 motoneurons after notch filtering. *E*: an average of individual cross-correlograms from consecutive swim cycles ( $n = 50$  correlograms). —, mean;  $\cdots$ ,  $\pm$ SD. In this case, the fast synaptic activities of the 2 cells were well correlated with a peak correlation coefficient of  $0.71 \pm 0.11$  occurring at a lag of 0 ms. All traces were low-pass filtered at 0.3 kHz.

The intracellular recordings initially were low-pass filtered with a cutoff frequency of 3.0 kHz (Axon Instruments, model 2130) and stored on an eight-channel DAT recorder (Biologic) for later off-line analysis. For the off-line analysis, the intracellular signals were further low-pass filtered and then digitized using a Cambridge Electronic Design (CED) 1401 computer interface, Spike2 software, and a 486 IBM-type computer. The analysis consisted of

performing cross-correlations of the synaptic activity in the motoneuron pairs. To correlate the fast synaptic activities of the cells, it was first necessary to remove the slow oscillations of fictive swimming from the membrane potential records; this would otherwise dominate the cross-correlograms. This was done using a digital notch filter provided by the Spike2 software, leaving the fast synaptic activity and action potentials (Fig. 1, B–D).

## Filtering

The digital notch filter implemented a finite impulse response filter consisting of 101 coefficients. The first data points of the waveform were multiplied by the coefficients and the result of the multiplications summed to produce an output data point. The set of coefficients then were shifted one step to the right and the process repeated. The peak of the notch filter was set as a fraction of the digitizing rate, and the same fraction (0.001) was used on all files. The swim frequency to be removed ranged in the different preparations from 0.6 to 2 cycles/s, mean =  $1.3 \pm 0.4$  (SD) cycles/s. Therefore the digitizing rate had to range from 0.6 kHz for the slowest swimming to 2 kHz for the fastest swimming. To ensure that the digitizing rate was sufficient to provide an accurate representation of the data (i.e., that the digitizing rate was at least twice the highest frequency components in the waveform), all recordings were low-pass filtered at 0.3 kHz before digitizing. This filter frequency was considered adequate to preserve the major frequency components of fast synaptic potentials because lamprey motoneurons have membrane time constants of  $\sim 10$  ms, as shown with step current injections (Buchanan 1993). Additional evidence for the adequacy of the 0.3-kHz filtering is that white-noise impedance measurements of motoneurons, done with a frequency range of 0.5–200 Hz, have been used to accurately simulate synaptic potentials using the inverse transform of the impedance function (Buchanan et al. 1992). Finally, tests of the dependence of the cross-correlations on the value of the low-pass filtering found only small changes in the peak amplitude of the cross-correlograms. For example (Fig. 2B), in a pair of motoneurons digitized at 2 kHz, the cross-correlation was compared when the data had been filtered at 0.3 versus 1.0 kHz. There was a nonsignificant 11% drop in the peak amplitude of the cross-correlation at 1.0 kHz compared with 0.3 kHz ( $P > 0.2$ , Student's *t*-test; Fig. 2B). It thus was concluded that the 0.3 kHz filter and the digitizing rate of at least two times this value were sufficient to preserve the character of the fast synaptic activity.

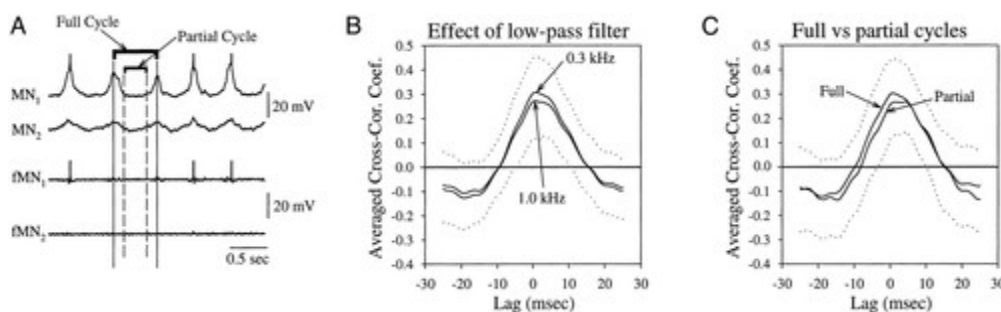


**Fig. 2.** Effect of low-pass filter frequency and windowing on the cross-correlations. A: sample of a paired intracellular recording between 2 motoneurons before notch filtering (*top 2 traces*, MN<sub>1</sub> and MN<sub>2</sub>) and after notch filtering (*bottom 2 traces*, fMN<sub>1</sub> and fMN<sub>2</sub>). Solid vertical lines, windowing for full swim cycles; dashed vertical lines, windowing of partial swim cycles. Data were sampled at 2.0 kHz. B: test of the effect of different low-pass filtering of the recordings before notch filtering. In this example, the recordings were filtered at a cutoff frequency of 1.0 kHz to compare with the usual cutoff frequency of 0.3 kHz. Cross-correlation coefficients were averaged ( $n = 50$ ) and the means are shown with solid lines. Dotted lines show the +SD for the 0.3-kHz mean and -SD for the 1.0-kHz mean. There was no significant difference in the peak coefficients ( $P > 0.2$ ). C: test of the effect of windowing on full swim cycles vs. partial swim cycles as illustrated in A. Shown are the mean cross-correlation coefficients for windowing on full swim cycles ( $n = 50$ ) and on partial swim cycles restricted to the repolarizing phase of the same recordings ( $n = 50$ ). Dotted lines show the +SD of the full cycle correlation

and the  $-SD$  for the partial cycle correlation. There was no significant difference in the peak coefficients ( $P > 0.2$ ).

## Data analysis

After the slow swim frequency was removed from the pair of waveforms with the notch filter, a cross-correlation was performed using a program written in the Spike2 script language that allowed averaging of multiple cross-correlograms (Fig. 1E). Averages were made on 50 consecutive swim cycles. When performing the cross-correlations, the more rostral motoneuron was used as the trigger and the caudal motoneuron as the reference. The cross-correlations were performed on windows of membrane potential activity that consisted of either a full or a partial swim cycle: if action potentials were absent in the records of both cells, a full swim cycle was used for the cross-correlation (peak depolarization to peak depolarization of 1 swim cycle, as assessed in prenotch filtered records displayed simultaneously with the notch-filtered records); if action potentials were present, the cross-correlations were made within windows between action potentials. High-gain records of the notch-filtered membrane potentials were used to place the window boundaries between action potentials, avoiding the slow afterhyperpolarization after the action potential. The afterhyperpolarizations were visible in the notch-filtered records, allowing placement of the beginning of the window at a point when the membrane potential had returned to its mean level. This tended to occur at a latency of  $\sim 50$  ms after the peak of the action potential. The end of the window was placed at a similar latency before the first action potential of the next cycle. These partial swim cycles were used exclusively in 51 pairs of motoneurons; full cycles were used exclusively in 5 pairs, and both full and partial cycles were used in 6 pairs. To assess whether there was any significant differences between full and partial swim cycle correlations, both types of analysis were done on three pairs of motoneurons (Fig. 2C). No significant differences were found between the peak cross-correlations using the two types of windowing ( $P > 0.2$ , Student's  $t$ -test). This finding suggests that the synaptic inputs occurring during the excitatory and inhibitory phases are correlated to similar degrees in given pairs of motoneurons. Therefore the results from these two windowing procedures were pooled.

The peak coefficient of the averaged correlograms is expressed as the mean  $\pm$  SD. The peak coefficient represents the maximum positive value found in the correlogram. For well-correlated records, the maximum value occurred at a distinct peak (Fig. 3, A3–D3). However, records with poor correlation often did not have distinct peaks (see Fig. 3E3). To provide a measure of the maximum positive values that would indicate a correlation, cross-correlations were done on noncorrelated data, that is, on pairs of motoneurons in which each member of the pair was recorded separately at different times ( $n = 3$ ). These correlograms had peak maximum values of 0.029, 0.045, and 0.052, respectively. Therefore peak coefficients  $< 0.06$  are not likely to be correlated.

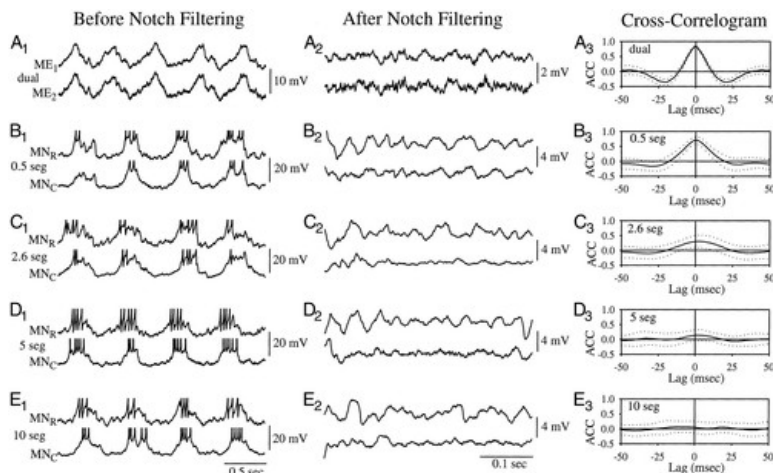


**Fig. 3.** Five examples of paired intracellular recordings from motoneurons during fictive swimming. *A*: dual-electrode recording in which 2 microelectrodes, ME<sub>1</sub> and ME<sub>2</sub>, were placed in the same motoneuron under visual guidance. *A1*: sample of the membrane potential oscillations before notch filtering is shown. *A2*: slow oscillations were removed with a digital notch filter, and the synaptic activity of 1 swim cycle is shown at higher gain. Note that some differences are clearly visible indicating differences in the filter characteristics of the electrodes and perhaps also in the ability of the electrodes to detect spatial differences in synaptic inputs to the cell. *A3*: cross-correlogram shows the averaged correlation coefficients (ACC) vs. lag. Peak correlation coefficient =  $0.83 \pm 0.04$  at 0 ms. *B*: pair of motoneurons located in the same ipsilateral segment and 0.5 segments apart (same pair as in Fig. 1). Peak correlation coefficient =  $0.71 \pm 0.11$  at 0 ms. *C*: pair of motoneurons separated by 2.6 segments. Peak correlation coefficient =  $0.31 \pm 0.21$  at 2.3 ms. *D*: pair of motoneurons separated by 5 segments. Peak correlation coefficient =  $0.14 \pm 0.19$  at 3.2 ms. *E*: pair of motoneurons separated by 10 segments. Peak correlation coefficient =  $0.07 \pm 0.19$  at -10.8 ms. All the illustrated cross-correlograms are averages of 50 consecutive swim cycles. — and ···, mean  $\pm$  SD. In all cases, the more rostral motoneuron was used as the trigger for the cross-correlation. All records were low-pass filtered at 0.3 kHz.

## RESULTS

When two motoneurons were located close to one another in the same spinal segment and on the same side of the spinal cord (Fig. 1A), the membrane potential activities of the two cells could be highly similar when recorded simultaneously with intracellular microelectrodes. The similarities were apparent both in the shapes of the slow swim cycle oscillations and in some details of the faster synaptic activities (Fig. 1B). After removal of the membrane potential oscillations of the swim cycle using a digital notch filter, the underlying fast synaptic activity could be seen more clearly. For the two motoneurons illustrated in Fig. 1, a highly similar pattern of synaptic activity was then apparent after notch filtering (Fig. 1C and D). Cross-correlation of the fast synaptic activity occurring in the portions of the swim cycle without action potentials revealed a high peak correlation coefficient between these two motoneurons (Fig. 1E; peak =  $0.71 \pm 0.11$ ). The high cross-correlation coefficient confirms and quantifies the impression that the two motoneurons have similar synaptic inputs during fictive swimming.

The highest peak correlation observed between two motoneurons was 0.74, indicating that there was never a perfect correlation of activity. Physiological factors certainly play a major role in this such as having similar but nonidentical sets of active premotor interneurons synapsing on the two motoneurons or because of the different electrophysiological properties of the two motoneurons [e.g., input resistances and membrane time constants (Buchanan 1993)]. However, nonphysiological factors also could play a role in limiting the degree of correlation such as differences in the filter characteristics of the two microelectrodes.

To provide some indication of the contribution of differences in the microelectrodes to the outcome of the cross-correlations, two microelectrodes were inserted into the same motoneuron during fictive swimming in two experiments (Fig. 3A). The peak coefficients of the averaged cross-correlations in these two-electrode recordings made from the same motoneuron ( $n = 2$ ) were 0.83 and 0.87, respectively. These values were higher than the peak coefficients observed with the microelectrodes in two separate motoneurons, but these values demonstrate that even with a two-electrode recording of a single cell, there was not a perfect correlation of the fast synaptic activity. It is likely that this difference is due in part to differences in the filter characteristics of the microelectrodes. However, there also appear to be real differences in the synaptic activity recorded by the two electrodes as revealed by close inspection of the high gain traces of Fig. 3A2. Thus although both electrodes were in the same motoneuron, they apparently could record differences in the spatial distributions of synaptic inputs to the cell. These dual-impalemt cross-correlation values place an upper limit on the peak correlation coefficients attainable using two microelectrodes and appear in Fig. 4 at the 0-distance point ( $\Delta$ ).



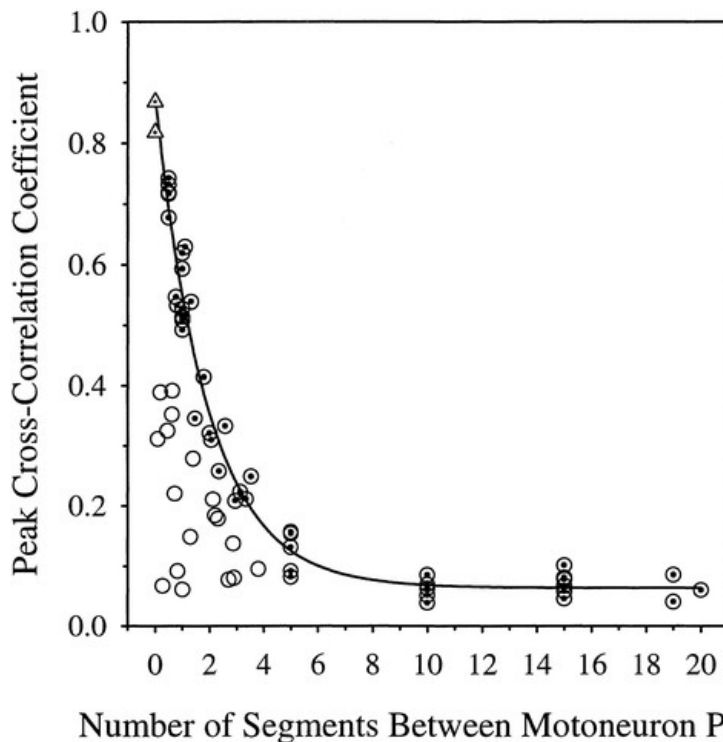


**Fig. 4.** Relationship between the peak of the averaged cross-correlation coefficients and the distance in spinal segments between the motoneurons. Two highest correlations ( $\Delta$ ) are from 2 motoneurons in which both microelectrodes were inserted into the same cell. These values give an indication of the maximum correlation obtainable with 2 microelectrodes. There was considerable variability in the peak correlations for different motoneuron pairs, which may reflect real differences in synaptic inputs to motoneurons even for those located in close proximity. It should be noted that the data for this plot were based mostly on correlations taken during the inhibitory phases to exclude action potentials from the cross-correlograms (see methods). To provide a measure of the relationship of the peak correlation coefficient with distance, a single exponential function was fitted to the higher correlations at each distance. ●, data points used for the fitted curve (46 of the 64 total points). Fitted curve is  $y = 0.81e^{x/1.9} + 0.064$ . Thus the length constant for the decrement of the correlation coefficient with distance was 1.9 spinal segments.

During fictive swimming, intracellular recordings were made among 62 pairs of motoneurons separated by various distances. The peak correlation coefficients of the cross-correlograms showed considerable variability, even for pairs of motoneurons located close to one another. For example, pairs of motoneurons located within two segments of one another had peaks that ranged from 0.06 to 0.74 (mean =  $0.44 \pm 0.20$ ,  $n = 29$ ; median = 0.49). Pairs of motoneurons located from two to four segments of one another had peaks that ranged from 0.08 to 0.33 (mean =  $0.20 \pm 0.08$ ,  $n = 14$ ; median = 0.21). At five segments and greater separating the motoneurons, the peaks ranged from 0.04 to 0.21 (mean =  $0.08 \pm 0.04$ ,  $n = 19$ ; median = 0.08). These means are significantly different from one another ( $P < 0.001$ , Student's *t*-test). The observation that motoneurons within the same segment may have a fairly high correlation (e.g., 0.7) or low or no correlation (0.06) suggests that motoneurons located within the same segment do not necessarily receive inputs from the same set of premotor interneurons. This suggests the existence of different functional groupings of myotomal motoneurons (see discussion).

In spite of the variability in the peak cross-correlation coefficients in pairs separated by similar distances, there was a clear decrease in the mean values of the peaks with the distance separating the motoneuron pairs. Individual examples of motoneuron pairs separated by various distances are shown in Fig. 3. The peak coefficients of the averaged cross-correlations were plotted versus the distance (in segments) between the pairs

of motoneurons in Fig. 4. It should be noted that the data for this plot were based mostly on correlations taken during the inhibitory phases to exclude action potentials from the cross-correlograms (see methods). There was a clear tendency for the peak coefficients to decrease with the distance separating the motoneurons. Beyond about five segments, little or no correlation remained. As described in the Methods, peak correlations of 0.03–0.05 were obtained when doing the cross-correlation analysis on noncorrelated cells (i.e., cells recorded separately at different times) and most of the pairs at distances more than five segments had peak correlations in this range, although 4 of the 14 cells had peaks between 0.08 and 0.10. For the smooth curve in Fig. 4, a single-exponential function was fit to the higher correlations at each distance ( $n = 44$  pairs, plus the 2 motoneurons recorded with dual impalements). The rationale for using the cells with the higher correlations at each distance is that if the variability in the peak correlations indicates different functional groupings of myotomal motoneurons, using those with the higher peaks allows a comparison of related motoneurons. The rationale for including the two motoneurons recorded with dual impalements in the curve is that these represent the maximum observed correlation obtained with two microelectrodes.

The peaks of the averaged correlograms often occurred at nonzero lags (Fig. 3, *C3* and *D3*); this could indicate that the correlated synaptic potentials tended to occur with a particular temporal relationship between the two motoneurons. One obvious factor that could contribute to nonzero lags would be the conduction time along common presynaptic axons. The relationship between the distance separating the motoneuron pairs and the offset of the peak correlation coefficient should then reveal the conduction velocity and the direction of propagation of the signals between the cells. However, as shown in Fig. 5, there was little or no correlation between the distance separating the motoneurons and the lag ( $R^2 = 0.25$ ;  $m = 0.9$  mm/ms). The data points used for Fig. 5 were those pairs of motoneurons separated by distances less than five segments that had sufficiently high correlations to determine the lag for the peak correlation coefficient. Most of the nonzero lags were positive (13 positive, 4 negative), which would be associated with rostral-to-caudal propagation of the signal.

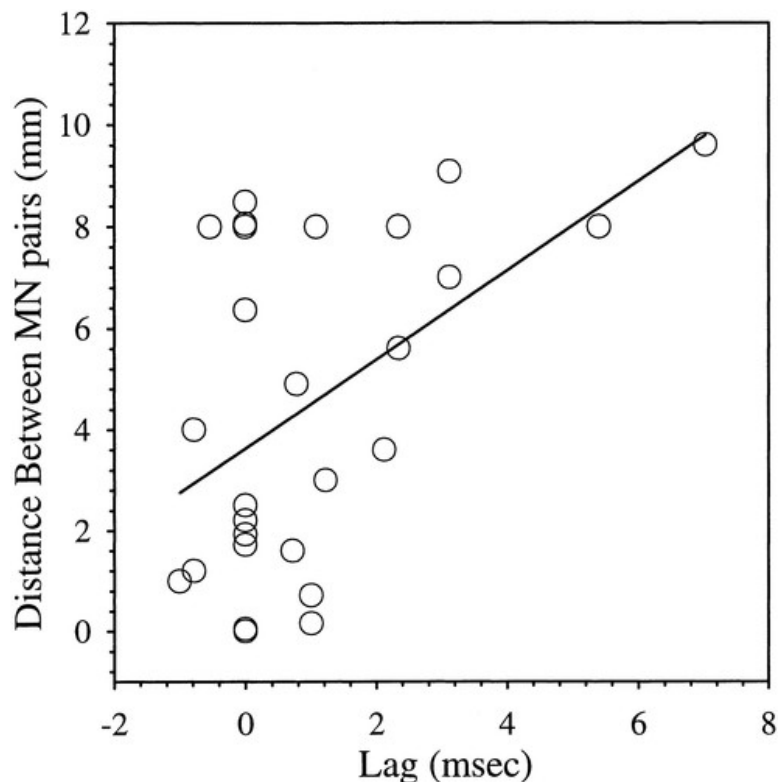


**Fig. 5.** Relationship of the distance between pairs of motoneurons and the lag of the peak correlation coefficient. Pairs of motoneurons chosen for the plot ( $n = 27$ ) were those with clearly discernable peaks in their averaged correlograms. Because the more rostral motoneuron was designated as the trigger in performing the cross-

correlations, positive lags represent a rostral-to-caudal delay. There is only a weak correlation between distance and lag ( $R^2 = 0.25$ ), but most lags are positive. Slope of the linear regression indicates a rostral-to-caudal propagation with a conduction velocity of 0.9 mm/s.

## DISCUSSION

During fictive swimming, the membrane potentials of motoneurons oscillate due to alternating phases of excitatory and inhibitory synaptic inputs (Buchanan and Cohen 1982; Buchanan and Kasicki 1995; Kahn 1982; Russell and Wallén 1983). It was shown in the present study that the synaptic potentials underlying these oscillations can be highly correlated between motoneurons located near one another within the same spinal segment. This result suggests that during fictive swimming, some neighboring motoneurons receive synaptic inputs from similar sets of premotor interneurons. Motoneurons separated by greater distances showed lower correlations of their synaptic activities, suggesting that their synaptic inputs come from different sets of premotor interneurons. The relationship between the correlation of synaptic activity versus the distance between the motoneurons (Fig. 4) indicates that the main region of influence of premotor interneurons is within about five spinal segments. This is a relatively short distance considering that the lamprey spinal cord contains ~120 spinal segments. Possible candidates for these local inputs are the excitatory interneurons, which have short ipsilateral axons (Buchanan et al. 1989), and the commissural interneurons with axons of less than five segments (Ohta et al. 1991), which may be predominately inhibitory (Buchanan 1982).

An interpretation of these experimental results is shown in Fig. 6. In this scheme, the spinal cord contains a continuous locomotor network, which can be reduced to about two or three segments as the minimal unit oscillator or CPG. Each unit CPG has a distributed set of outputs that are strongest to the motoneurons of the same segment and progressively weaker in rostral and caudal directions (Fig. 6A). Therefore a given motoneuron will not only receive input from its local CPG but also from more distant CPGs. Two motoneurons in the same segment will have a high correlation of synaptic activity because they both receive strong inputs from the same CPG interneurons. Two motoneurons located in different segments will have a lower correlation of synaptic activity because their strongest inputs will be originating from different sets of CPG premotor interneurons. But because of the distributed nature of the CPG outputs, the two motoneurons will have some overlapping inputs (compare MN<sub>3</sub> and MN<sub>5</sub> in Fig. 6B), and thus will still show some correlation. However, because the strengths of the CPG outputs decline with distance, the local inputs to each of these motoneurons located in different segments will be strong and uncorrelated and will tend to obscure the weaker correlated inputs to the two cells.

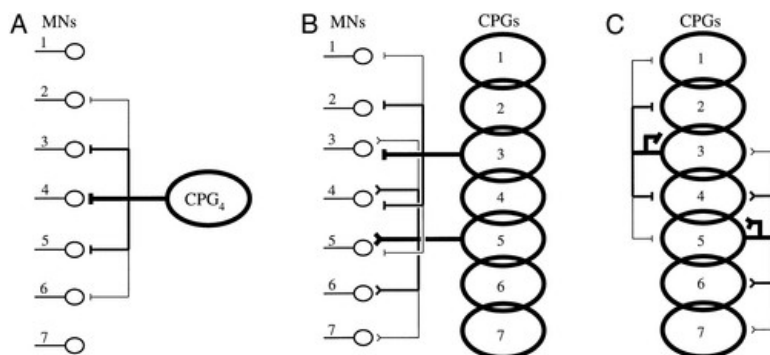


**Fig. 6.** Model for the spatial distribution of common inputs to pairs of motoneurons. Spinal cord contains a series of overlapping central pattern generators (CPGs) responsible for generating the basic alternating swim rhythm in motoneurons (MNs). Minimal length that will generate rhythmic activity is 2–3 segments. A: each unit CPG provides strong excitatory and inhibitory outputs to nearby motoneurons. These same signals go to motoneurons in other segments, but with strengths that decrease with distance from the segment of origin (indicated by thinner connecting lines). Results of the present study suggest that the spread is limited to only a

few segments in either direction. *B*: because the spinal cord contains a chain of unit CPG oscillators and each CPG has distributed outputs, the motoneurons of 1 segment will receive excitatory and inhibitory inputs not only from the local CPG but also from adjacent CPGs. Cross-correlations therefore are strongest between pairs of motoneurons in the same segments. For example, 2 MNs of segment 3 will have a higher correlation than a MN of segment 3 vs. a MN of segment 5. Because motoneurons that are separated by >5 segments show little correlation, the strengths (or numbers) of the nonlocal connections must fall quickly with distance. *C*: because the interneurons of the proposed locomotor network synapse on motoneurons and also among themselves, it is proposed that the same populations of interneurons generate the basic locomotor rhythm, provide output to the motoneurons, and provide the coupling among the unit CPGs. This would suggest that the interoscillator coupling signals are predominantly via nearest-neighbor connections.

The premotor interneurons that provide the output to motoneurons during fictive swimming also synapse among themselves to form the proposed unit oscillator (Buchanan 1982; Buchanan and Grillner 1987; Buchanan et al. 1989). Therefore it is our working hypothesis that the same set of locomotor interneurons is responsible not only for providing output to motoneurons, but also for rhythm generation and for interoscillator coupling (Fig. 6C). The feasibility of this scheme has been demonstrated with computer simulations of the network (Buchanan 1992; Williams 1992). This hypothesis would predict that paired recordings between locomotor interneurons, i.e., CC interneurons, excitatory interneurons, and lateral interneurons, would yield correlations that vary with distance in a manner similar to motoneurons. The alternative hypothesis is that the outputs from the unit CPGs have different distribution lengths depending on their targets. It is possible, for example, that the CPG outputs to motoneurons are short while the CPG outputs to other CPG interneurons are longer. This scheme would perhaps help to stabilize the rostral-to-caudal phase coupling of the oscillators but allow for more local control of the motoneurons. This hypothesis would predict that paired recordings between locomotor interneurons would show a longer length constant than that found for motoneurons in Fig. 4.

In the present study, cross-correlations between motoneurons separated by more than five segments showed low correlations (range = 0.04–0.10). Tests on noncorrelated data gave peak correlations coefficients of <0.06 (see methods), so many of these motoneuron pairs separated by more than five segments showed no significant correlations. However, these results do not exclude the existence of intersegmental signals longer than five segments but suggest that such long-range connections are much weaker than the short-range connections. There are several experimental studies in lamprey demonstrating the existence of long-range signals. For example, in lesion studies of the lamprey spinal cord during fictive swimming, shortening of the spinal cord to three segments reduced the synaptic drive in motoneurons to ~30% of the value recorded in the 18-segment preparation before shortening (Wallén et al. 1993). This finding suggested that the summated synaptic inputs from more distant segments were stronger than the local synaptic inputs. However, these experiments probably underestimated the local synaptic drive because spinal cord lengths less than four segments are only marginally capable of generating regular rhythmic activity (Cohen and Wallén 1980). Thus the observed reduction in synaptic drive may have simply reflected a depressed state of the local generator rather than the loss of more distant premotor inputs. In another study, modeling of correlations among ventral root discharges suggested that long-range coupling exists (Mellen et al. 1995). Additional evidence for long-range coupling has been obtained using three-bath experiments in which a middle region of the spinal cord is inhibited by application of glycine or low-calcium solutions. In these experiments, coupling of fictive swimming could be maintained across inhibited spinal cord  $\leq 20$  segments in length (Miller and Sigvardt 1996; Rovainen 1985). Some interneurons of the proposed locomotor network have axons projecting 30–50 spinal segments (Buchanan 1982; Rovainen 1974), so the anatomic substrate for long-range connections exists. In the present experiments, some of the motoneuron pairs separated by 10–20 segments may have shown weak correlations (0.08–0.10). The higher correlations at these distances may be due to input from inhibitory CC interneurons, some of which have been

shown to project  $\leq 30$  segments and synapse directly on motoneurons (Buchanan 1982). Thus although it is likely that pairs of motoneurons separated by more than five segments will receive some common inputs, the cross-correlation technique used here does not readily demonstrate them. The presumed reason for this is that these distant inputs are only small contributors to the total synaptic drive. It would be predicted that these distant common synaptic inputs would be demonstrated easily with this cross-correlation technique in a quiescent preparation.

The wide range of peak correlation coefficients between pairs of motoneurons located even within the same segment (Fig. 4) suggests that some motoneurons receive significantly different inputs during fictive swimming in spite of their close proximity. It has been shown previously that motoneurons in the same segment, but innervating muscles located at different dorsoventral levels of the body, can show different oscillatory patterns during fictive swimming (Wallén et al. 1985). In particular, motoneurons innervating the midline part of a myotome tended to show different oscillatory patterns than motoneurons innervating the lateral part of a myotome. The midline-innervating motoneurons also have dendrites that cross the midline of the spinal cord while the laterally innervating motoneurons do not. It then would be expected that midline-innervating motoneurons would receive inputs from different sets of premotor interneurons compared with laterally innervating motoneurons. The wide range of cross-correlations between close pairs of motoneurons therefore may indicate functional differences among motoneurons and may imply that the unit locomotor oscillator is fractionated into components related to different dorsoventral levels of the body.

The estimate of conduction velocity of the intersegmental signals from the plot of distance versus the offset of the peak correlation coefficients suggested a caudally projecting signal with a conduction velocity of 0.9 mm/ms (Fig. 5). Although conclusions cannot be made from the weak relationship of Fig. 5, it is interesting to note that this conduction velocity is consistent with the conduction velocities of medium-sized interneurons such as CC interneurons, which have caudally projecting axons (Buchanan 1982). The lack of a strong relationship between distance and the offset is not surprising. Motoneurons receive both ascending and descending signals (Dale 1986), which would result in both phase leads and phase lags of synaptic potentials in the more caudal motoneuron. In the cross-correlograms this mixture of phase relations would tend to obscure phase relations due to particular populations of ascending or descending neurons. To make a clearer distinction between the contributions of ascending versus descending signals, it would be possible to perform a split-bath experiment in which a diffusion barrier separates the bath into independently-perfused pools with fictive swimming occurring in only the rostral or the caudal half of the preparation. In this way, it would be possible to separately examine the correlations associated with ascending versus descending signals (Dale 1986). This might also reveal longer coupling signals because the mixture of phase leads and lags may degrade the correlations, especially in widely separated cells.

Several factors may contribute to the lengths of intersegmental coupling signals: the average lengths of the axons involved in coupling, how the number of synaptic outputs are distributed along the lengths of the axons (e.g., more frequent axonal outputs close to the cell body vs. at a distance), and how the synaptic strengths are distributed along the lengths of the axons (e.g., stronger connections close to the cell body of origin vs. at a distance). Although the present study does not address the anatomic and physiological determinants of coupling strength, it does give an overall measure of the functional lengths of intersegmental signals from the unit CPG for fictive swimming to the motoneurons. These signals appear to be relatively short, characterized mainly as nearest-neighbor in length.

Our thanks to T. Strauss for help with data analysis.

This work was supported by National Institute of Neurological Disorders and Stroke Grants NS-28369 and NS-35725 to J. T. Buchanan and National Institutes of Health Fogarty Central and Eastern Europe Senior Fellowship in the Neurosciences 5 F05 TW04648 to S. Kasicki.

Present address of S. Kasicki: Dept. of Neurophysiology, Nencki Institute of Experimental Biology, 3 Pasteura, 02-093 Warsaw, Poland.

## FOOTNOTES

- The costs of publication of this article were defrayed in part by the payment of page charges. The article must therefore be hereby marked “*advertisement*” in accordance with 18 U.S.C. Section 1734 solely to indicate this fact.

## AUTHOR NOTES

- Address for reprint requests: J. T. Buchanan, Dept. of Biology, Marquette University, P.O. Box 1881, Milwaukee, WI 53201-1881.

## REFERENCES

- 1 Buchanan J. T. Identification of interneurons with contralateral, caudal axons in the lamprey spinal cord: synaptic interactions and morphology. **J. Neurophysiol.** 47:1982-961 (1975)
- 2 Buchanan J. T. Premotor interneurons in the lamprey spinal cord: morphology, synaptic interactions, and activities during fictive swimming. **Neurobiology of Vertebrate Locomotion**, Grillner S., Stein P.S.G., Stuart D. G., Forssberg H., Herman R. M. 1986:321-334 MacMillan London
- 3 Buchanan J. T. Neural network simulation of coupled locomotor oscillators in the lamprey spinal cord. **Biol. Cybern.** 66:199-236 (1974)
- 4 Buchanan J. T. Electrophysiological properties of identified classes of lamprey spinal neurons. **J. Neurophysiol.** 70:1993-2313 (1975)
- 5 Buchanan J. T., Cohen A. H. Activities of identified interneurons, motoneurons, and muscle fibers during fictive swimming in the lamprey and effects of reticulospinal and dorsal cell stimulation. **J. Neurophysiol.** 47:1982-948 (1960)
- 6 Buchanan J. T., Grillner S. Newly identified “glutamate interneurons” and their role in locomotion in the lamprey spinal cord. **Science** 236:1987-3123 (1974)
- 7 Buchanan J. T., Grillner S., Cullheim S., Risling M. Identification of excitatory interneurons contributing to generation of locomotion in lamprey: structure, pharmacology, and function. **J. Neurophysiol.** 62:1989-5969
- 8 Buchanan J. T., Kasicki S. Activities of spinal neurons during brain stem -dependent fictive swimming in lamprey. **J. Neurophysiol.** 73:1995-8087
- 9 Buchanan J. T., Moore L. E., Hill R., Wallén P., Grillner S. Synaptic potentials and transfer functions of lamprey spinal neurons. **Biol. Cybern.** 67:1992-1231 (1971)
- 10 Cohen A. H., Ermentrout G. B., Kiemel T., Kopell N., Sigvardt K. A., Williams T. L. Modeling of intersegmental coordination in the lamprey central pattern generator for locomotion. **Trends Neurosci.** 15:1992-434 (1992)
- 11 Cohen A. H., Wallén P. The neuronal correlate of locomotion in fish. “Fictive swimming” induced in an in vitro preparation of the lamprey spinal cord. **Exp. Brain Res.** 41:1980-1118
- 12 Dale N. Excitatory synaptic drive for swimming mediated by amino acid receptors in the lamprey. **J. Neurosci.** 6:1986-2662 (1975)
- 13 Grillner S., Buchanan J. T., Lansner A. Simulation of the segmental burst generating network for locomotion in lamprey. **Neurosci. Lett.** 89:1988-3135
- 14 Grillner S., Deliagina T., Ekeberg Ö., El Manira A., Hill R. H., Lansner A., Orlovsky G. N., Wallén P. Neural networks that co-ordinate locomotion and body orientation in lamprey. **Trends Neurosci.** 18:1995-2702 (1995)

- 15 Grillner S., Wallén P., Brodin L., Lansner A. Neuronal network generating locomotor behavior in lamprey: circuitry, transmitters, membrane properties, and simulation. *Annu. Rev. Neurosci.* 14:1991-169200
- 16 Kahn J. A. Patterns of synaptic inhibition in motoneurons and interneurons during fictive swimming in the lamprey, as revealed by Cl<sup>-</sup> injections. *J. Comp. Physiol.* 147:1982-189194
- 17 Mellen N., Kiemel T., Cohen A. H. Correlational analysis of fictive swimming in the lamprey reveals strong functional intersegmental coupling. *J. Neurophysiol.* 73:1995-10201030
- 18 Miller W. L., Sigvardt K. A. Influence of multisegmental coordinating fibers on rhythmicity of distant segments in the lamprey spinal central pattern generator. *Soc. Neurosci. Abstr.* 22:1996-1642
- 19 Ohta Y., Dubuc R., Grillner S. A new population of neurons with crossed axons in the lamprey spinal cord. *Brain Res.* 564:1991-143148
- 20 Perrins R., Roberts A. Cholinergic contribution to excitation in a spinal locomotor central pattern generator in *Xenopus* embryos. *J. Neurophysiol.* 73:1995-10131019
- 21 Rovainen C. M. Synaptic interactions of identified nerve cells in the spinal cord of the sea lamprey. *J. Comp. Neurol.* 154:1974-189206
- 22 Rovainen C. M. Effects of groups of propriospinal interneurons on fictive swimming in the isolated spinal cord of the lamprey. *J. Neurophysiol.* 54:1985-959977
- 23 Russell D. F., Wallén P. On the control of myotomal motoneurons during "fictive swimming" in the lamprey spinal cord in vitro. *Acta Physiol. Scand.* 117:1983-161170
- 24 Wallén P., Ekeberg O., Lansner A., Brodin L., Tråvén H., Grillner S. A computer-based model for realistic simulations of neural networks. I. The segmental network generating locomotor rhythmicity in the lamprey. *J. Neurophysiol.* 68:1992-19391950
- 25 Wallén P., Grillner S., Feldman J. L., Bergelt S. Dorsal and ventral myotome motoneurons and their input during fictive locomotion in lamprey. *J. Neurosci.* 5:1985-654661
- 26 Wallén P., Lansner A. Do the motoneurons constitute a part of the spinal network generating the swimming rhythm in the lamprey. *J. Exp. Biol.* 113:1984-493497
- 27 Wallén P., Shupliakov O., Hill R. H. Origin of phasic synaptic inhibition in myotomal motoneurons during fictive locomotion in the lamprey. *Exp. Brain Res.* 96:1993-194202
- 28 Wallén P., Williams T. L. Fictive locomotion in the lamprey spinal cord in vitro compared with swimming in the intact and spinal animal. *J. Physiol. (Lond.)* 347:1984-225239
- 29 Williams T. L. Phase coupling by synaptic spread in chains of coupled neuronal oscillators. *Science* 258:1992-662665
- 30 Williams T. L., Sigvardt K. A., Kopell N., Ermentrout G. B., Remler M. P. Forcing of coupled nonlinear oscillators: studies of intersegmental coordination in the lamprey locomotor central pattern generator. *J. Neurophysiol.* 64:1990-862871